Draft version July 14, 2021
Typeset using LaTeX manuscript style in AASTeX63

Ion cloud expansion after hypervelocity dust impacts detected by the MMS electric probes in the dipole configuration

Jakub Vaverka,[1] Jiří Pavlů,[1] Libor Nouzák,[1] Jana Šafránková,[1] Zdeněk Němeček,[1] Tarjei Antonsen,[2] Ingrid Mann,[2] and Per-Arne Lindqvist[3]

[1] Faculty of Mathematics and Physics, Charles University, Prague, Czech Republic

[2] The Arctic University of Norway, Tromsø, Norway

[3] Royal Institute of Technology, Stockholm, Sweden

(Received January 25, 2021; Revised January 25, 2021; Accepted July 14, 2021)

Submitted to ApJ

ABSTRACT

The dust impact detection by electric field instruments is already a well-established technique. On the other hand, not all aspects of signal generation by dust impacts are completely understood and explained. We present a study of events related to dust impacts on the spacecraft body detected by electric field probes operating simultaneously in the monopole (probe-to-spacecraft potential measurement) and dipole (probe-to-probe potential measurement) configurations by the Earth-orbiting Magnetospheric Multiscale mission (MMS) spacecraft. This unique measurement allows us to investigate connections between monopole and dipole data. Our analysis shows that the signal detected by the electric field instrument in a dipole configuration is generated by ion cloud expanding along electric probes. In this case, expanding ions affect not only the potential of the spacecraft body but also one or more electric probes at the

Corresponding author: Jakub Vaverka
jakub.vaverka@mff.cuni.cz

end of antenna booms. Electric probes located far from the spacecraft body can be influenced by ion cloud only when the spacecraft is located in tenuous ambient plasma inside of the Earths magnetosphere. Derived velocities of the expanding ions in order of tens km·s^{-1} are in the range of values measured experimentally in the laboratory.

Keywords: Ion cloud expansion — Hypervelocity dust impacts — Spacecraft charging

1. INTRODUCTION

Dust grains impacting with high velocities onto the spacecraft body can be partly or totally evaporated together with a small part of the spacecraft material and create a plasma cloud. The electrons and ions in the hypervelocity impact plasma can consequently influence the spacecraft potential and/or measurements of scientific instruments onboard. It has been shown that electric field instruments are able to register signals generated by dust impacts as short pulses in the measured electric field. The first detection of such pulses has been reported from the Voyager spacecraft during a crossing of Saturns ring plane (Aubier et al. 1983; Gurnett et al. 1983). This method is recently used for dust detection by many missions in various parts of our Solar system such as Deep Space 1 (Tsurutani et al. 2004), Cassini (Wang et al. 2006; Kurth et al. 2006; Ye et al. 2014, 2016, 2019), Wind (Malaspina et al. 2014; Wood et al. 2015; Malaspina & Wilson 2016), STEREO (Meyer-Vernet et al. 2009; Zaslavsky et al. 2012; Zaslavsky 2015; Malaspina et al. 2015; Kellogg et al. 2016; O'Shea et al. 2017), MAVEN (Andersson et al. 2015), Cluster (Vaverka et al. 2017b,a), MMS (Vaverka et al. 2018, 2019) and Parker Solar Probe (Szalay et al. 2020; Page et al. 2020).

The configuration of the electric field instruments is very important for dust impact detection and understanding of the measured signal (Meyer-Vernet et al. 2017; Vaverka et al. 2018). The instrument operating in the monopole configuration (probe-to-spacecraft measurement) where the spacecraft body is used as reference electrode are sensitive to changes of the spacecraft potential generated by dust impacts. On the other hand, instruments operating in the dipole configuration are only sensitive to the influence of the expanding cloud of charged particles or to asymmetrical potential in the spacecraft surrounding mainly for non-balanced dipole antennas (Malaspina et al.

2014). The mechanism of the dust impact signal generation and its consequent detection by the electric field instruments in the monopole configuration is comprehensively described by Mann et al. (2019).

Vaverka et al. (2018) illustrated the difference between the signal of dust impact and that generated by a solitary wave detected by multiple electric field instruments simultaneously in dipole and monopole configurations. Dust impacts, contrary to solitary waves, generate signals mainly in data measured in the monopole configuration. Nevertheless, Vaverka et al. (2018) found that dust impact on the spacecraft body can generate a signal on electric probes located far aways ($\sim$ 14 m) from the spacecraft but the exact mechanism of the generation of this signal is not clear. Zaslavsky (2015) suggested that some fraction of the charged particles can be recollected by the antenna/probe and can result in such pulses. On the other hand, O'Shea et al. (2017) have shown that the recollection of charged particles by electric field antennas is extremely ineffective and thus Vaverka et al. (2018) speculated that the antenna signal detected by the MMS spacecraft can be generated by the potential of the ion cloud expanding along the electric probes without recollection of expanding particles. The generation of antenna signal by the potential of the ion cloud was also studied by (Nouzák et al. 2018; Mann et al. 2019; Shen et al. 2021). Some of the spacecraft are equipped only with electric field instruments operating only in the dipole configuration as Wind or Cluster and other missions use primarily the dipole configuration as Cassini or Parker Solar Probe. It is therefore important to understand the dust impact onto the spacecraft body, the subsequent processes and the signal they generate in the instruments operating in dipole configuration.

We use data from one of the MMS spacecraft (MMS1) with focus on pulses which were attributed to dust impacts in previous work (Vaverka et al. 2019) and focus on events that were detected in monopole and dipole configuration. We study these events in detail to understand mechanisms of dust impact detection in these configuration and to validate the ion cloud expansion hypothesis suggested by Vaverka et al. (2018). We utilise a simple model to estimate the possible effect of expanding ion cloud on dipole measurements and investigate direct influence of the spacecraft potential on electric probes.

2. MMS SPACECRAFT

The four Magnetospheric Multiscale mission (MMS) spacecraft are orbiting the Earth in a close formation since 2015 in highly elliptical orbits (Burch et al. 2016). Each of these spacecraft is equipped with three pairs of electric field probes, two in the spin plane - probes P1-P4 ($\sim$ 120 m tip-to-tip) (Lindqvist et al. 2016; Torbert et al. 2016) and one shorter pair in the axial direction - probes P5 and P6 ($\sim$ 30 m) (Ergun et al. 2016; Torbert et al. 2016). The important fact is that only tips of the booms are used as sensors (probes). This is a crucial difference from electric field antennas where a whole antenna element is active and it has important implications for registration of dust impacts. The tips of booms are spheres (8 cm in diameter) for spin plane double-probes and tubes (2,25 m long and 0.64 cm in diameter) for axial probes. The advantage of this instrument is that it operates nearly simultaneously in both monopole and dipole configurations. The monopole is sensitive to changes of the spacecraft potential while the dipole is susceptible to changes in the ambient electric field or to changes in the potential of dipole probes. As the distance of the electric field sensors from the spacecraft body is well defined for both types of dipole probes, it provides a new important view on the interpretation of data. The simultaneous measurement in both configurations allows us to compare and discuss individual events detected in both regimes. This comparison can provide very interesting information about dipole signal obtained by other spacecraft where it is not possible to match this signal with the monopole data.

3. DUST IMPACT AND IMPACT CLOUD EXPANSION

The processes behind dust impact onto a solid surface and consequent dust/surface evaporation are not yet completely understood. **The impact** ionization process have been studied in laboratory conditions e.g. by (Auer 2001; Collette et al. 2015, 2016). The hypervelocity dust impacts generate a plasma cloud expanding away from the spacecraft body. Frequent collisions lead to thermalization of electrons but the plasma plume becomes very quickly collisionless due to its expansion. One can speculate that the fraction of electrons recollected by the spacecraft thus would depend on the duration of the initial collisional phase but survey of results on this topic (Meyer-Vernet et al. 2017) as well as latest experiments at the dust accelerator (Shen et al. 2021) revealed that about a half of electrons moving backward to the spacecraft. Electrons and ions decouple from the original plume (Meyer-Vernet et al. 2017; Mann et al. 2019; Nouzák et al. 2020, 2021) and are later influenced by the spacecraft potential and/or electric field in the spacecraft surrounding (Collette et al. 2015; Nouzák et al. 2018; Mann et al. 2019). The motion of electrons can be also affected by the presence of a magnetic field, as in the case of the Cassini spacecraft Grand Finale (Nouzák et al. 2020). It should be noted that the sunlight illuminated spacecraft in the solar wind at 1 AU or in the Earth's magnetosphere are typically charged positively because the photoemission is a dominant charging process in these environments (Vaverka et al. 2017a). The positively charged spacecraft attracts electrons back to the spacecraft body and repels positive ions. The efficiency of this separation depends on the energy (temperature) of the electrons/ions and on the spacecraft potential. A majority of the electrons could be recollected when the positive spacecraft potential is significantly higher than the energy of cloud electrons. The recollection of electrons (escape of ions) results in a decrease of the positive spacecraft potential and consequent relaxation to the equilibrium value is due to interactions with ambient plasma and photoemission. It should be noted that the impact plasma cloud is conductively connected with the spacecraft in the initial phase of expansion. A notable change of the spacecraft potential thus can occur with a delay needed for the sufficient cloud expansion (Meyer-Vernet et al. 2017). Temporal variations in the spacecraft potential can be detected as identical pulses seen by all electric field probes operating in the monopole configuration. On the other hand, the signal generated by changes in the ambient environment like solitary waves results in different pulses (including opposite polarity) on monopole probes oriented in different directions (Vaverka et al. 2018).

The amplitude of a voltage pulse in the monopole data (the disturbance of the spacecraft potential from the equilibrium value) is given by a total charge of recollected particles from the impact plasma and spacecraft capacitance. The charge recollected by the spacecraft body is equal to the total charge of particles leaving the spacecraft in the expanding plasma cloud divided by the spacecraft capacitance that is about 110 pF for MMS spacecraft.

4. EVENT IDENTIFICATION

The identification of dust impacts in the measured electric field could be a very challenging issue mainly in environments with the low dust flux and with a presence of natural electric waves as, for example, in the Earth-orbit. False positive events can significantly influence the obtained results in this case. In previous works (Vaverka et al. 2018, 2019), a method was developed to identify dust impacts in the MMS multiple electric field probes data. To summarize, this method uses the fact that the changes in the spacecraft potential result in identical pulses with the same polarity in all monopole probes and identifies impacts by the automatic code using correlation coefficients for signals from two pairs of monopole probes. Events with correlation coefficients higher than 0.9 for opposite probes were considered as candidates for dust impacts and later visually inspected.

An example of a typical event related to a change of the spacecraft potential is shown in the left panel of Figure 1 (adopted from Vaverka et al. (2019)). The top panel shows the probe-to-spacecraft potential measurements, P, the middle panel shows the electric field measurements in a dipole configuration, E, and the bottom panel shows the spacecraft potential derived from the monopole data, U_{sc}. Six identical pulses in the monopole data (top panel) and no or very small pulses in the dipole signal (middle panel) show that this event is related to a change in the spacecraft potential. An automatic routine described by Vaverka et al. (2019) detected 363 similar events corresponding to changes in the spacecraft potential in burst mode data from MMS1 in the year 2016. Some of these events contain also a signal (including very small pulses) in the short dipole (axial double probe).

The Figure 1 shows an example of one pulse with a dipole component on its right side (adopted from Vaverka et al. (2018)). It is possible to see that one of the pulses in the monopole configuration (P5) is enhanced, and dipole (E56) registered a higher signal. It has been mentioned that Vaverka et al. (2018) speculated that this signal can be generated by expansion of the escaping ion cloud along the electric field probe, thus the potential of the probe (P5) can be influenced by the positive potential of the ion cloud expanding along the electric probe. It results in the detected dipole signal and in the enhancement of the monopole (probe-to-spacecraft) signal. In such a case, five monopoles

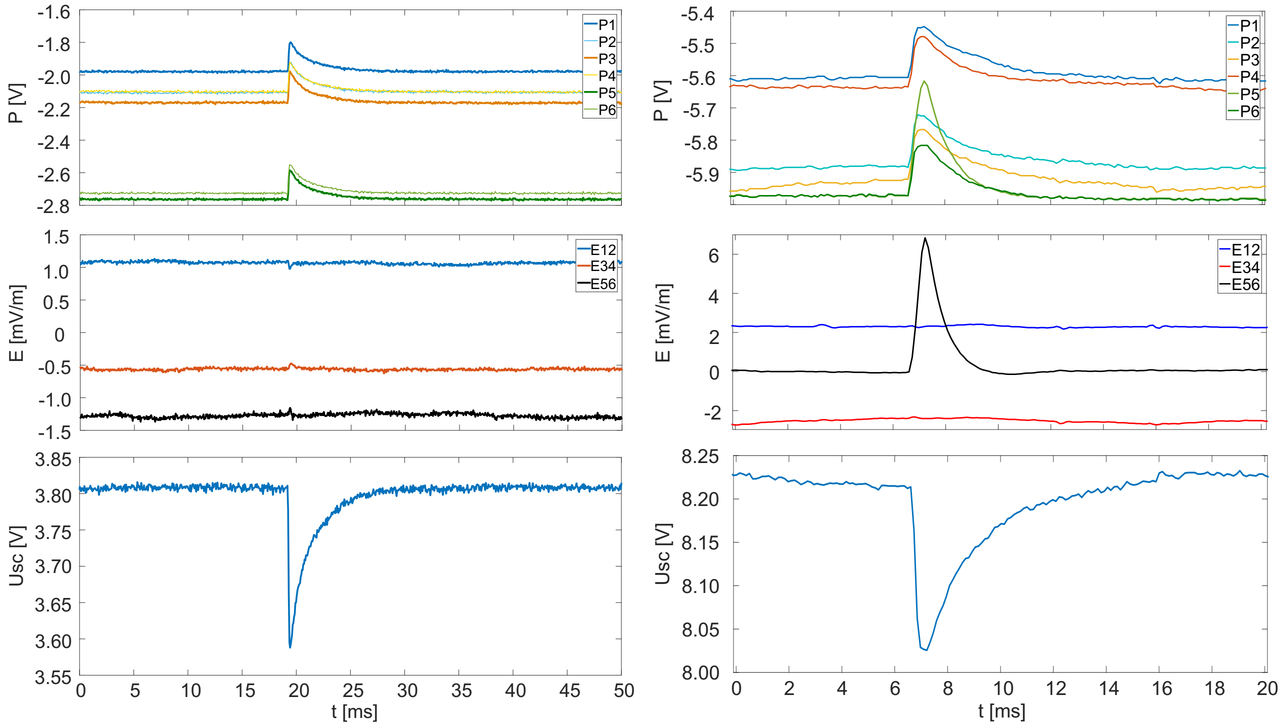

Figure 1. The example of a typical event related to the change of the spacecraft potential (candidate for a dust impact) selected by the automatic routine. Probe-to-spacecraft potential measurement, P (top), the electric field measurement in the dipole configuration, E (middle), and the spacecraft potential derived from the monopole data, U_{sc} (bottom), left (adopted from Vaverka et al. (2019)). Example of a similar event with a signal recorded by short (14 m) dipole, right (adopted from Vaverka et al. (2018)).

register only a change of the spacecraft potential but the signal registered by the probe P5 is the sum of the spacecraft potential change and potential of the probe influenced by the expanding ion cloud.

A detailed study shows that from detected 363 pulses in the spacecraft potential 155 (43 %) events contain a signal in the short dipole (E56) located 14 m from the spacecraft body and 74 (20 %) events are registered by one or both longer dipoles (E12 and/or E34) located 60 m from the spacecraft body. The analysis of these events is presented in the following sections.

5. RESULTS AND DISCUSION

5.1. *Signal shape - expansion velocity*

An example of an event exhibiting pulses in three dipoles is shown in Figure 2. It should be noted that similar events are relatively rare. The electric field pulse measured by a short dipole (E56) is typically significantly higher than that for longer dipoles (E12 and E34). Generally, the maxima of the amplitude in monopoles and dipoles are reached at different times and the polarity of dipole signals is not necessarily identical. It indicates that the signal detected in the dipole is not just crosstalking from the monopole. The pulses are both positive and negative for all three dipoles with an approximately similar probability. Assuming the cloud expansion scenario, the polarity of the pulse depends on which probe of the particular dipole is influenced by the expanding ion cloud. The equal presence of both polarities suggests that the expanding ion cloud reaches both probes from the same dipole in a similar number of cases. This follows naturally for dipoles E12 and E34 from the spacecraft rotation (3.1 RPM). On the other hand, the axial double probe (E56) is still at the identical north-south orientation. It means that ion clouds expand with a similar probability up or down along the spin axis of the spacecraft (there is no significant difference in numbers of dust grains impinging from the north/south directions).

It is possible to see a small overshoot on the dipole E56 in Figure 2. Similar overshoots are present for the majority of cases. The important fact is that the amplitudes of overshoots are independent on the amplitudes of main pulses. The overshoot can be as high as the main pulse but there are also events with no overshoot. It is necessary to point out that the comprehensive explanation of these overshoots is unknown, although similar overshoots can result from the amplifier response to the initial pulse caused by the limited bandwidth as in the case of Cassini Ye et al. (2019). However, such explanation is probably not applicable on MMS data because the occurrence of these overshoots is strongly irregular. We suggest that the formation of the second pulse with opposite polarity could result from expansion of the ion cloud along both electrical probes of the same dipole at different times. Since the expanding cloud is able to reach the tip of long dipole ($\sim$ 60 m), it can easily reach both tips of a short dipole.

Observations shown that the maximum value is first reached by short dipole (E56) for all cases. This is consistent with our hypothesis that this signal is connected to the ion cloud propagation from the spacecraft body. The average time needed to reach a maximum value is (0.67 ± 0.06) ms for a short antenna and (1.87 ± 0.16), respectively (1.86 ± 0.15) ms for long dipoles. This time is measured

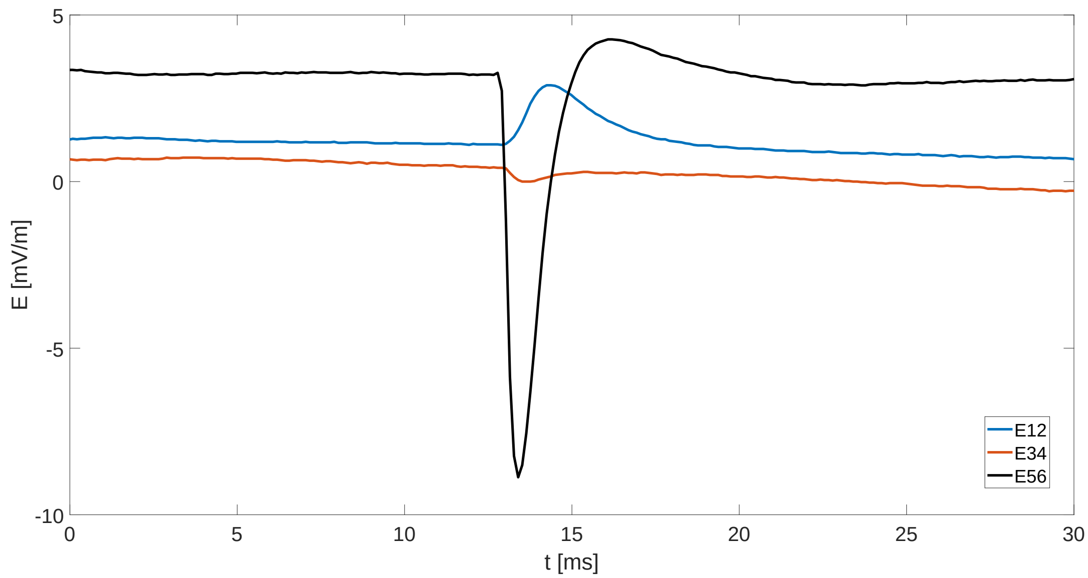

Figure 2. The example of one event containing pulses in all three dipoles.

from the beginning of a pulse in the monopole to the maximum in a dipole signal. It is necessary to mention that the beginning of the pulse in the monopole data is not exactly the time when the plasma cloud leaves the spacecraft body Meyer-Vernet et al. (2017). It is possible to use these times and lengths of the particular dipoles to roughly derive the velocity of expanding ions. The average value of the ion expanding velocity detected by the short dipole (E56) is (21 ± 2) km·s^{-1}. The obtained velocity for the dipoles E12 and E34 are (32 ± 3) km·s^{-1}. These uncertainties are derived from statistical distribution of expansion times. The higher average velocities detected by longer dipoles could be the result of the acceleration of positive ions from the positively charged spacecraft or/and by different nature of expansion in these two significant directions (parallel and perpendicular after impact in ecliptic plane). The obtained velocities are in the range of values measured experimentally by Lee et al. (2012) and it supports our ion cloud expansion hypothesis.

5.2. *Influence of ambient plasma environment*

The surprising fact that the expanding ion cloud reaches the electric probes located 14 m or even 60 m from the spacecraft body could be explained by the low density of the ambient plasma in the magnetosphere. We can compare the impact cloud propagation under various conditions because the

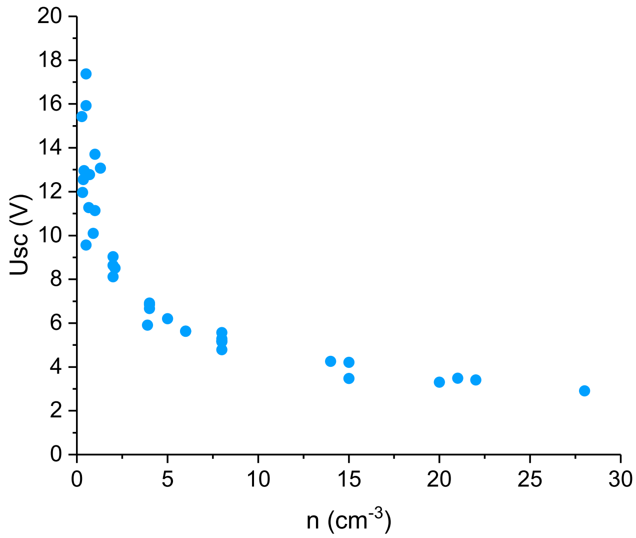

Figure 3. The spacecraft potential, U_{SC} as a function of the electron density, n.

MMS spacecraft cross regions with different plasma densities. The information about the ambient plasma is unfortunately not available in the regions where the plasma density is too low. On the other hand, the spacecraft potential depends on the plasma density (Vaverka et al. 2017a) and can be used as a proxy of electron fluxes (Pedersen et al. 2008; Andriopoulou et al. 2018). The spacecraft potential, U_{SC} as a function of the electron density, n for several dust impacts is shown in Figure 3. These electron densities have been obtained by Fast Plasma Investigation (Pollock et al. 2016). The spacecraft potential monotonically increases with decreasing electron density because the photoemission becomes more dominant in tenuous plasma environments. The MMS potentials can reach values up to 40 V, significantly higher than those shown in the figure. It is possible to expect that these extreme potentials are connected to environments with plasma density significantly lower than 1 cm^{-3} that can be encountered in magnetospheric lobes.

The left panel of Figure 4 shows a histogram of all dust impacts detected in the monopole configuration as well as events registered simultaneously in dipole configurations for probes located 14 and 60 m from the spacecraft body as a function of the spacecraft potential, U_{SC}. The distribution of the events in the monopole configuration is given by a spacecraft motion through the Earth's magnetosphere. It is possible to see that the number of events detected by the short dipole (gray) is higher than that for a longer boom (white) for all values of the spacecraft potential. The probability of the signal detection by the dipole rises with spacecraft potential (decreasing electron density). The reason is that the expanding plasma cloud can be absorbed by the ambient plasma if its density is sufficiently high. The electric probe can detect signal only when the potential of expanding ions is not shielded by the surrounding plasma. The probabilities of the signal detection by dipoles are shown in the right panel of Figure 4 as a function of the spacecraft potential. The pulses are simultaneously detected at least by one dipole approximately in 10 % of cases only when the spacecraft potential is lower than 5 V. This corresponds to the electron density higher than 5 cm^{-3} (see Figure 3). It means that dust detection by a similar electric field instrument as onboard MMS in the dipole configuration is inefficient under solar wind and magnetosheath conditions. The efficiency significantly increases for very low plasma densities, below 1 cm^{-3} where the expanding plasma cloud is dense enough to reach the electric probes.

The total charge of expanding ion cloud, Q could be roughly derived from the change of the spacecraft potential, dU_{SC} as $Q = dU_{SC} \cdot C$, where C is spacecraft capacitance (section 3). The accuracy of this estimation can be limited by discharging effect of ambient plasma (reduction of dU_{SC}), by efficiency of the charge separation, or by the mutual capacitance between the antenna and the spacecraft. In the first approximation, we can consider that the charge is uniformly distributed in a expanding sphere of radius, R. The radius of such cloud at the moment when when its density is equal to the density of the ambient plasma is shown in Figure 5 as a function of ambient plasma density, n for several values of dU_{SC} (0.01, 0.1, 1, and 10 V). We should note that this radius is used only to compare the density of the plasma cloud with the ambient plasma and does not represent a hard threshold where the plasma cloud has no effect on the electric probe. It is possible to see that diameter of the sphere of uniformly distributed charge corresponding to values detected in the monopole configuration can reach tens of meters before its density decreases to the density of the tenuous magnetospheric plasma and thus even long dipoles can register dust impacts in this environment. On the other hand, the size of such a sphere is only a few meters under the solar wind

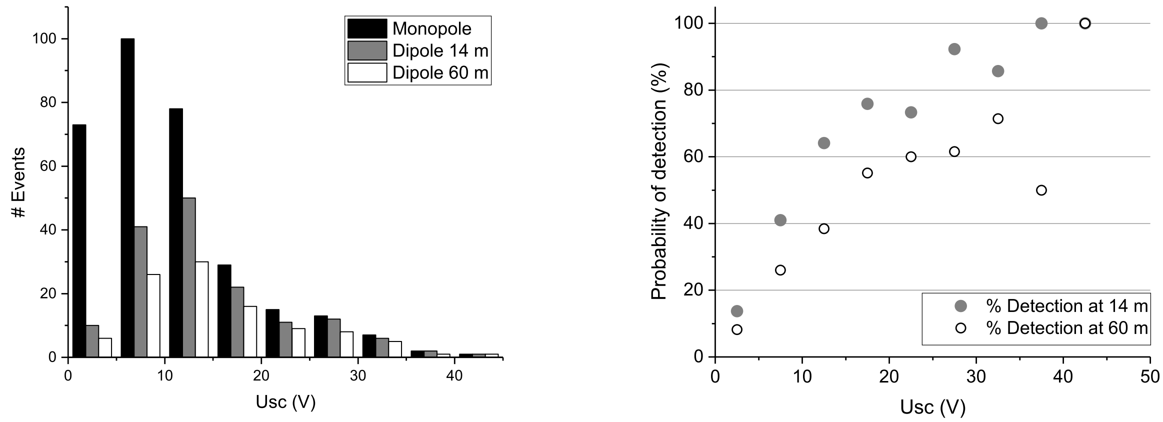

Figure 4. The number of events detected in monopole and dipole configurations for probes located 14 and 60 m from the spacecraft body as a function of the spacecraft potential, U_{SC} (left panel). The probability of signal detection by dipole probes as a function of the spacecraft potential (right panel).

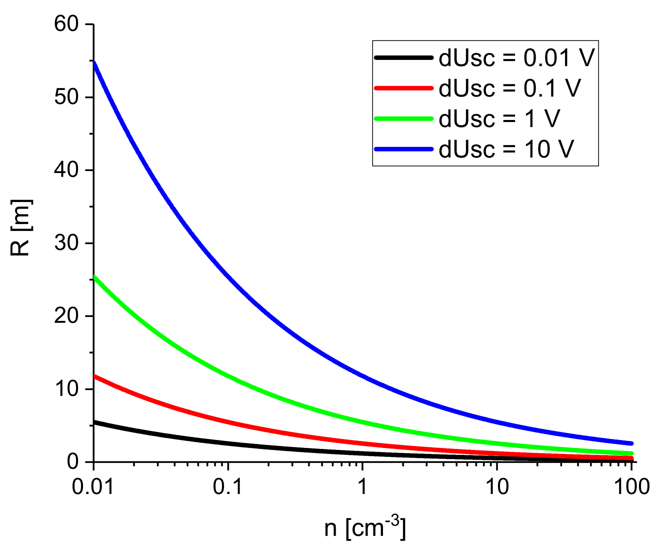

Figure 5. The radius of the ion spherical cloud, R under assumption that the density of uniformly distributed escaping ions is equal to the density of the plasma as a function of the ambient plasma density, n for several values of changes in the spacecraft potential, dU_{SC} (total charge in the cloud).

conditions. This explains the dependence of the dust detection efficiency in dipole configuration on the ambient plasma density.

5.3. *Amplitude of the signal*

A very important question is if the cloud expanding along the electric probe is able to generate signals measured in the dipole configuration. The detailed analysis of the expanding ion cloud structure and its influence on the electric probes is far behind the scope of this study but we can apply a simple model to roughly estimate the amplitude of the dipole signal corresponding to the pulse in the spacecraft potential. We assume that the ion cloud expands as a sphere with increasing effective radius. Although such spherical approximation is far from the real situation it allows us to estimate the electric potential inside of this sphere and to derive signal corresponding to the measured electric field from the length of the particular dipole. We can apply two different scenarios, in the first scenario (fast expansion), the effective radius of the expanding sphere increases with the same rate as the distance from the spacecraft and in the second one (slow expansion), the radius increases ten times slower (sphere reaches radius 1 m at distance of 10 m from the spacecraft body). A simple sketch of these two situations is shown in Figure 6 (fast expansion - red spacecraft, slow expansion - blue spacecraft). The signal detected by the dipole by such a cloud is given by the potential inside this sphere (charge in the sphere and its size) and by the length of the dipole. Figure 7 shows the signal estimated by this simple model of spherical cloud expansion for the short (E56 left panel) and for long (E12 and E34 right panel) dipoles as a function of the change of the spacecraft potential, dU_{SC} together with the measured electric field during dust impacts (data points). The model for fast expansion (the first scenario) is plotted by a red line and the model for slow expansion (the second scenario) by the blue line. The amplitude of the measured pulses in the electric field increases with dU_{SC} supports our hypothesis of ion cloud expansion. It is possible to see that the majority of measured points is located between our two scenarios. It shows that the expanding ion clouds of a total charge corresponding to pulses in a monopole data are theoretically able to generate similar pulses as those detected in the dipole configuration.

5.4. *Influence of the spacecraft potential on dipole measurements*

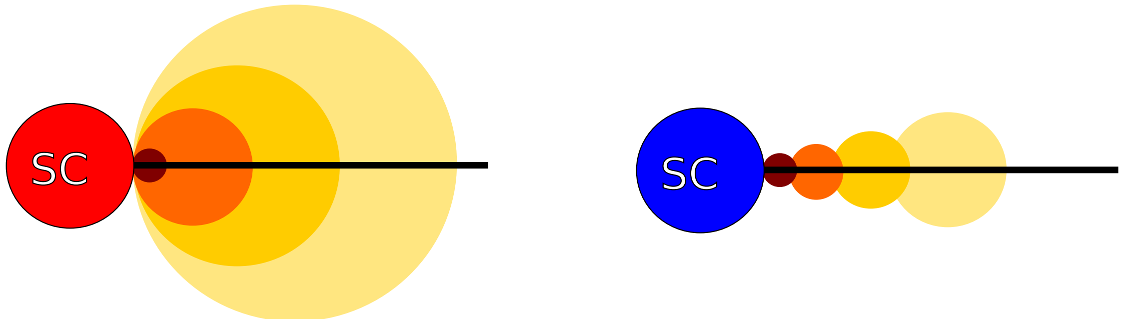

Figure 6. The sketch of the simple model of ion cloud expansion. Fast expansion scenario is shown on the left panel and slow expansion scenario is on the right panel.

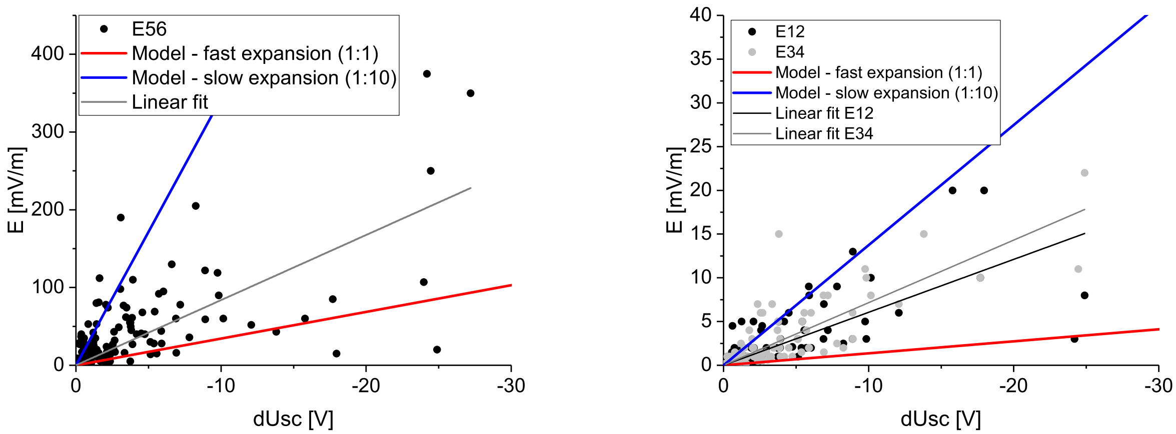

Figure 7. The electric field measured during dust impacts (data points) and corresponding signal estimated by a simple model of the spherical cloud expansion (Figure 6) for the short dipole E56 (left panel) and for long dipoles E12 and E34 (right panel) as a function of the pulse in the monopole data, dU_{SC} (change of the spacecraft potential). The model for the fast expansion is plotted by the red line and the model for slow expansion by the blue line.

In previous section, we discussed the generation of a dipole signal by the potential of expanding charge. Another mechanism has been proposed by (Malaspina et al. 2014) for WIND. The disturbance in the spacecraft potential caused by dust impact could affect both probes/antennas of the dipole in a different way and this asymmetrical influence can lead to a measurable signal in the dipole configuration. It is important to note that the identical influence on both dipole arms does not result in a measurable signal. The reason for the asymmetry could be different effective lengths of both dipole arms as in the case of WIND when one of the antennas has been shortened (Malaspina et al. 2014) or different environments at both antennas resulting in a different shielding length. The non-uniform environment around the spacecraft can be caused by the presence of the photoelectron sheath at the UV illuminated part of the spacecraft. This can be a case of the MMS like spacecraft when one of the spin plane probes can be shielded by a photoelectron sheath and the second one can be in the spacecraft shadow. It is necessary to mention that this effect is more significant for probes located closer to the spacecraft body than in MMS (60 m) or for electric antennas where a whole antenna element is electrically sensitive. The strongest effect of the asymmetrical conditions occurs when one end of the dipole is completely shielded from the influence of the spacecraft potential and the effect on the second one is reduced only by the geometrical factor $1/r$, where r is the distance from the spacecraft body. An application of such extreme condition on the MMS dipole for the spacecraft potential disturbance 1 V results in the dipole signal 2.8 mV/m for the short dipole and 0.14 mV/m for longer ones. The significantly larger disturbance in the spacecraft potential, 20 V results in the dipole signals 56 mV/m respectively 2.8 mV/m. This extreme case corresponds approximately to the red line in fast expansion scenario in Figure 7. It is possible to see that the direct effect of the spacecraft potential on MMS dipole measurements is much weaker than the measured signal shown in Figure 7 and it is not possible to explain measured pulses by the effect of the asymmetric influence of the spacecraft potential. It is important to note that maxima of the dipole and monopole signals occur at the identical time in the case of the asymmetrical influence of the spacecraft potential. Our study shows that maxima are reached at different times by monopole and dipole instruments. It indicates that the measured dipole signal is not a result of this effect.

It has been mentioned that the asymmetric influence of the spacecraft potential is significantly stronger for short distances from the spacecraft than in case of MMS. We can estimate the expected dipole signal measured under different conditions assuming shielding by factor $e^{-\frac{r}{\lambda_d}}$, where λ_d is a shielding length. Figure 8 shows the dipole signal caused by this asymmetry as a function of the electric probe distance from the spacecraft body for various environments and different lengths of antenna arms caused by 1 V disturbance in the spacecraft potential. The solid lines show the situation when both probes are in different environments represented by different shielding lengths.

Black line represents shielding lengths 1 and 10 m, blue line 1 and 100 m, grey line 10 and 100 m, and green line represents a situation when one probe is totally shielded from the effect of the spacecraft potential and the influence on the second one is reduced only by the geometrical factor $1/r$. The dashed lines represent the situation when one probe of the dipole is 20 % closer to the spacecraft for three shielding lengths (100 m, black line, 10 m, red line, and 1 m, grey line). The dash-dot-dot lines show a similar situation when one probe is 50 % closer to the spacecraft for the same shielding lengths as in the previous case.

One can see that the signal strongly decreases with the distance of the probe from a spacecraft body. The 1 V pulse in the spacecraft potential is only able to generate the signal close to 1 mV/m for probes located 20 m from the spacecraft. The strongest field is generated for the cases when one probe is strongly shielded by an ambient plasma and the second one is shielded very weakly (black, blue, and green solid lines). The strong effect can be also observed when one probe is significantly closer (50 %) than the second one (black and red dash-dot-dot lines).

It is necessary to mention that this figure is valid for cases when the location of the electric field sensor is well defined as in MMS. The situation of the electric field antennas is much complex and this figure provides only qualitative information for such cases.

6. SUMMARY AND DISCUSSION

Pulses detected in the dipole configuration after hypervelocity dust impacts onto the spacecraft body are probably caused by the expansion of the ion cloud along the electric probe. There are several indications supporting this hypothesis:

- The different timing of signal in the monopole and dipole configuration indicate that the dipole signal is not just a cross-talk from monopole channel.
- A polarity of the pulse in the dipole configuration is random (there are a similar number of positive and negative pulses). This is possible to explain by the spacecraft rotation for dipoles in spin plane (E12 and E34) and by no significant deflection of incoming dust grains from the ecliptic plane for dipole E56.

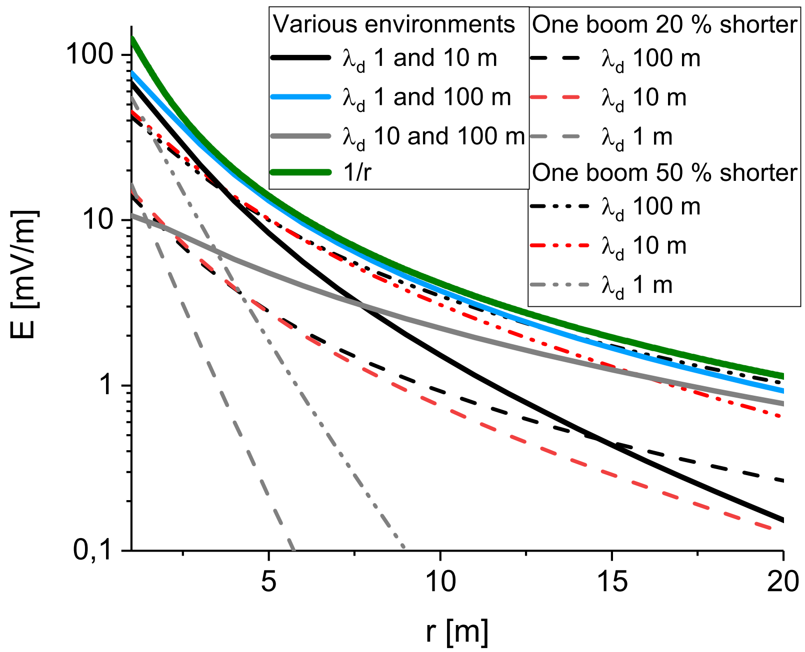

Figure 8. The dipole signal caused by the asymmetrical influence of the 1 V disturbance in the spacecraft potential on the electric probes in the dipole configuration as a function of the electric probe distance from the spacecraft body. The solid lines show the situation when both probes are in different environments represented by different shielding lengths. The green line represents a situation when one probe is totally shielded from the spacecraft potential and the influence on the second one is reduced only by the geometrical factor $1/r$. The dashed lines represent the situation when one probe is 20 % closer to the spacecraft body for three different shielding lengths and the dash-dot-dot lines shown a similar situation when one probe is 50 % closer to the spacecraft body.

- Only a fraction of the monopole pulses is accompanied by dipole signal and the short dipole detects more events than the longer ones.

- Probability of signal detection in dipole configuration depends on the spacecraft potential (density of ambient plasma). Dipole signal is detected mainly in environments with low ambient plasma density.

- The peak of the pulse is first reached by the short dipole (E56) in the case when the signal is simultaneously detected by several dipoles.

- The derived velocities of expanding ions correspond to values measured in the laboratory by Lee et al. (2012).

- Based on our simple model, the total generated impact charge derived from the monopole pulses can also generate pulses with the amplitudes detected in the dipole configuration.

- It is not possible to explain the measured dipole signal by the direct asymmetric effect of the spacecraft potential on the electric field measurements as suggested by (Malaspina et al. 2014).

The effect of the asymmetrical influence of the spacecraft potential on the electric probes is very weak for probes located far from the spacecraft body. On the other hand, this effect can be important for electric antennas where the whole surface is electrically sensitive. One of the antenna booms should be significantly shorter then the second one or one of the antennas should be in different plasma environment as in the wake of spacecraft or in the photoelectron sheath to obtain measurable signal. In this case, the dipole signal generated by dust impacts on the spacecraft body can be a combination of both effects, the influence of escaping ion cloud and asymmetric effect of the spacecraft potential.

It is necessary to mention that the presence of overshoots remains unexplained. The fact that the amplitude of overshoots is independent on the initial pulse (some pulses are without overshoots at all) indicates that the response of instrumental electronics is not the source of these overshoots. The overshoots could be explained by the expansion of the ion cloud along both electric probes of the dipole but there is no experimental support for this hypothesis.

7. CONCLUSION

We have analysed 363 pulses in the spacecraft potential caused by hypervelocity dust impacts onto the body of the MMS1 spacecraft during the year 2016. 155 of these events are accompanied with pulses in the electric field measured by the axial probe (short dipole) located 14 m from the spacecraft body and 74 of these events result in signal measured by one or both spin plane double probes (long dipoles) located 60 m from the spacecraft.

We have shown that the probability of signal detection in a dipole configuration depends on the density of ambient plasma (Figure 4). Several indications support our hypothesis that signal detected in the dipole configuration is caused by a cloud of ions escaping from the positively charged spacecraft body.

We have shown that the charge in the ion cloud is large enough to generate pulses of detected amplitudes in the measured electric field (Figure 7) and that the effect of the asymmetrical influence of the spacecraft potential on the electric probes is very weak for probes located far from the spacecraft body (Figure 8). Both effects, influence of escaping ion cloud and asymmetric effect of the spacecraft potential should be taken into account when investigating dust impacts detected by electric antennas.

Derived velocities of escaping ions are (21 ± 2) km·s^{-1} for short dipole and (32 ± 3) km·s^{-1} for long dipoles. These velocities are in the range of values measured experimentally in the laboratory by Lee et al. (2012). The higher average velocities detected by longer dipoles could be a result of the acceleration of positive ions by the positively charged spacecraft or/and by different nature of expansion in these two significant directions (parallel and perpendicular after impact in ecliptic plane).

ACKNOWLEDGMENTS

This work was supported by Czech ministry of education youth and sport under contract LTAUSA 17066 and by the Czech Science Foundation under Project 20-13616Y. IM and TA are supported by the Research Council of Norway (grant number 262941). We acknowledge the Magnetospheric MultiScale (MMS) development, operations, and science teams. The data used in this paper were provided by the MMS Science Data Center. The authors thank to ISSI (International Space Science Institute) in Bern for organizing of the meeting which discussions within the working group Physics of Dust Impacts: Detection of Cosmic Dust by Spacecraft and its Influence on the Plasma Environment contributed to complementation of this paper.

REFERENCES

Andersson, L., Weber, T. D., Malaspina, D., et al. 2015, Science, 350

Andriopoulou, M., Nakamura, R., Wellenzohn, S., et al. 2018, J. Geophys. Res. Space Physics, 123, 2620

Aubier, M. G., Meyer-Vernet, N., & Pedersen, B. M. 1983, Geophysical Research Letters, 10, 5

Auer, S. 2001, Springer, 385

Burch, J. L., Moore, T. E., Torbert, R. B., & Giles, B. L. 2016, Space Sci. Rev., 199, 5

Collette, A., Malaspina, D. M., & Sternovsky, Z. 2016, J. Geophys. Res. Space Physics, 121, 8182

Collette, A., Meyer, G., Malaspina, D., & Sternovsky, Z. 2015, J. Geophys. Res. Space Physics, 120, 5298

Ergun, R. E., Tucker, S., Westfall, J., et al. 2016, Space Sci. Rev., 199, 167

Gurnett, D. A., Grün, E., Gallagher, D., Kurth, W. S., & Scarf, F. L. 1983, Icarus, 53, 236

Kellogg, P. J., Goetz, K., & Monson, S. J. 2016, J. Geophys. Res. Space Physics, 121, 966

Kurth, W. S., Averkamp, T. F., Gurnett, D. A., & Wang, Z. 2006, Planet. Space Sci., 54, 988

Lee, N., Close, S., Lauben, D., Linscott, I., & Goel, A. e. a. 2012, Int. J. Impact Eng., 44, 40

Lindqvist, P., Olsson, G., Torbert, R. B., et al. 2016, Space Sci. Rev., 199, 137

Malaspina, D. M., Horanyi, M., Zaslavsky, A., et al. 2014, Geophys. Res. Lett., 41, 266

Malaspina, D. M., O'Brien, L. E., Thayer, F., Sternovsky, Z., & Collette, A. 2015, J. Geophys. Res. Space Physics, 120, 6085

Malaspina, D. M., & Wilson, L. B., I. 2016, J. Geophys. Res. Space Physics, 121, 9369

Mann, I., Nouzak, L., Vaverka, J., Antonsen, T., & Fredriksen, A. e. a. 2019, Ann. Geophys., 37, 11211140,

Meyer-Vernet, N., Moncuquet, M., Issautier, K., & Schippers, P. 2017, J. Geophys. Res. Space Physics, 122, 8

Meyer-Vernet, N., Maksimovic, M., Czechowski, A., et al. 2009, Solar Physics, 256, 463

Nouzák, L., James, D., Němeček, Z., et al. 2021, Astrophys. J., 909, 132, doi: 10.3847/1538-4357/abd6e7

Nouzák, L., Sternovsky, Z., Horanyi, M., et al. 2020, J. Geophys. Res. Space Phys., 125, e2019JA027245, doi: 10.1029/2019JA027245

Nouzák, L., Hsu, S., Malaspina, D., et al. 2018, Planet. Space Sci., 156, 85

O'Shea, E., Sternovsky, Z., & Malaspina, D. M. 2017, J. Geophys. Res. Space Physics, 122, 11864

Page, B., Bale, S. D., Bonnell, K. W., Goetz, K., & et al., G. K. 2020, ApJS, 246

Pedersen, A., Lybekk, B., Andr, M., et al. 2008, J. Geophys. Res. Space Physics, 113

Pollock, C., Moore, T., Jacques, A., et al. 2016, Space Sci. Rev., 119, 331

Shen, M. M., Sternovsky, Z., Horanyi, M., Hsu, H.-W., & Malaspina, D. M. 2021, J. Geophys. Res. Space Phys., 126

Szalay, J. R., Pokorny, P., Bale, S. D., et al. 2020, ApJS, 246

Torbert, R. B., Russell, C. T., Magnes, W., et al. 2016, Space Sci. Rev., 199, 105

Tsurutani, B. T., Clay, D. R., Zhang, L. D., et al. 2004, Icarus, 167, 89

Vaverka, J., Pavlu, J., Nouzak, L., et al. 2019, J. Geophys. Res. Space Phys., 124, 8179

Vaverka, J., Pellinen-Wannberg, A., Kero, J., et al. 2017a, IEEE Trans. Plasma Sci., 45, 2048

—. 2017b, J. Geophys. Res. Space Phys., 122, 6485

Vaverka, J., Nakamura, T., Kero, J., et al. 2018, J. Geophys. Res. Space Phys., 123, 6119

Wang, Z., Gurnett, D. A., Averkamp, T. F., Persoon, A. M., & Kurth, W. S. 2006, Planet. Space Sci., 54, 957

Wood, S. R., Malaspina, D. M., Andersson, L., & Horanyi, M. 2015, J. Geophys. Res. Space Physics, 120, 7121

Ye, S., Gurnett, D. A., Kurth, W. S., et al. 2014, J. Geophys. Res. Space Physics, 119, 3373

Ye, S., Kurth, W. S., Hospodarsky, G. B., Averkamp, T. F., & Gurnett, D. A. 2016, J. Geophys. Res. Space Physics, 121, 11,964

Ye, S., Vaverka, J., Nouzak, L., et al. 2019, Geophys. Res. Lett., 46, 10,941

Zaslavsky, A. 2015, J. Geophys. Res. Space Physics, 120, 855

Zaslavsky, A., Meyer-Vernet, N., Mann, I., et al. 2012, J. Geophys. Res. Space Physics, 117